PROCEEDINGS, 41st Workshop on Geothermal Reservoir Engineering
Stanford University, Stanford, California, February 22-24, 2016
SGP-TR-209

Numerical Simulation of Mixed Brine-CO_2/H_2S-Rock Interaction During the Reinjection of Non-condensable Gases

Alex Grey M. Saldaña[1], Eylem Kaya[1]*, Sadiq J. Zarrouk[1], Victor Callos[1], Bruce W. Mountain[2]

[1]Department of Engineering Science, University of Auckland, Private Bag 92019, Auckland 1142, New Zealand
[2]GNS Science, Wairakei Research Centre, New Zealand

*e.kaya@auckland.ac.nz

Keywords: non-condensable gases, NCG, CO_2 sequestration, geochemical reactions, fluid-rock interaction geothermal reservoir modeling, TOUGHREACT

ABSTRACT

There is an increased interest in the reinjection of non-condensable gases (NCG) from geothermal power stations into geothermal reservoirs. NCG reinjection can serve as a means of reducing greenhouse gas emissions into the atmosphere, provide reservoir pressure support and possibly can be considered a stimulation method to improve reservoir permeability. Reservoir modeling studies are essential in understanding the behavior of injected gases in the reservoir and forecast possible NCG breakthrough to production wells. The NCG can be injected either as dissolved gas in water or as supercritical fluid. This paper aims to determine how a geothermal reservoir rock will behave during injection of a representative mixture of CO_2/H_2S-water injection.

A laboratory scale flow-through experiment was conducted to investigate the complex interaction between CO_2/H_2S-brine and greywacke rock sample. By introducing detailed reactive chemistry into the injected liquid mixture and mineral composition, this study simulates the conditions of the experiment, and attempts to quantify the fluid-rock interactions for a better understanding of the impact of NCG reinjection on the reservoir porosity and permeability. This is to assess the potential use of long and short term NCG reinjection in conventional geothermal systems. Reasonable match was obtained between experimental data and geochemical modeling using the TOUGHREACT simulator. The simulation study showed that all the reactions are taking place very fast at reservoir temperature, indicating thermodynamically-controlled reactions (equilibrium).

1. INTRODUCTION

Geothermal fluid contains variable quantity of NCG, consisting primarily of CO_2, H_2S, N_2, NH_3, H_2, and CH_4. The total gases can be as high as 15% by weight of the total fluid extracted. The presence of NCG, in particular CO_2 and H_2S, in the geothermal fluids often presents a challenge as these are associated with corrosion, calcite deposition, reduced power plant efficiency, and health, safety, and environmental risks (Papic, 1991; DiPippo, 2012).

The NCG are accumulated in the geothermal power plant condenser, hence the name is NCG, and have to be extracted. These gases are conventionally extracted and discharged to the atmosphere using some of the generated power.

CO_2 is the dominant NCG, making up to about 90% of the total gases in most geothermal systems (Truesdell, 1979; Mahon, 1980). The major sources of CO_2 may be from magmatic origins, sedimentary formations, organic matter, and shallow bicarbonate springs. CO_2 is also associated with the occurrence of hydrothermal calcite deposition near-wellbore through the following equilibrium reaction (Satman et al., 1999):

$$Ca^{2+} + 2HCO_3^- \leftrightarrow CaCO_3 \downarrow (\text{deposition}) + H_2O + CO_2 \uparrow \quad (1)$$

With the exsolution of CO_2 from the geothermal fluids such as by boiling in the hot up-flow region of the reservoir or rapid degassing such as in a vertical geyser vent or a in production well, the forward reaction is favored and calcite deposits (Simmons and Christenson, 1994; Jones and Renaut, 1998).

Hydrogen sulfide, on the other hand, is a flammable, reactive and toxic gas, which can cause possible life-threatening risks. Sulfur dioxide (SO_2) is a known component of acid rain, results as an oxidation product of H_2S.

Reinjection of CO_2 into geothermal reservoirs is receiving increasing interest from many industries to minimize the emission of the greenhouse gas into the atmosphere and to extend the productive life of geothermal reservoirs through pressure support. The presence of CO_2 in the reservoir fluid lowers the flash point pressure of the mixed fluid and promotes boiling. This will induce the formation of a gas phase in the geothermal reservoir, and in the process help maintain higher total reservoir pressures. Injected CO_2 could be in the form of supercritical state or dissolved in water (brine). Injection of CO_2 with brine is preferred over single phase CO_2 injection since it enhances geochemical reaction rates and increases reservoir permeability. This method also decreases the risk of gas leakage due to reduced buoyancy effects and formation damage caused by high injection pressures of supercritical fluid.

The mineral alteration induced by injection of CO_2 can lead to changes in porosity. Furthermore, co-injecting H_2S can cause additional porosity changes in the acidified zones where mineral dissolution dominates, e.g. the reaction of ferrous iron with dissolved sulfide can form pyrite:

$$Fe^{2+} + 2HS^- \leftrightarrow FeS_2 \text{ (pyrite)} + 2H^+ + 2e \quad (2)$$

NCG reinjection has been applied to geothermal reservoirs, with a variable success, in few fields including: Hijiori, Japan (Yanagisawa, 2010); Ogachi, Japan (Kaieda et al., 2009); Hellisheidi Iceland, (Alfredsson and Gislason, 2009), Coso, (Nagl, 2010; Sanopoulos and Karabelas, 1997) and Puna (Richard, 1990). At Hijiori, Ogachi, and Hellisheidi, CO_2 was dissolved in water at very low concentrations (0.01 to 3 % by weight) prior to injection. The Coso Geothermal field has been accepting dissolved NCG in the reinjection water but later switched to H_2S removal system due to reduced reservoir performance (Nagl, 2009). Pilot-scale experiments have also been conducted in the Hellisheidi and Nesjavellir power plants in Iceland to assess the feasibility of in-situ sequestration of both CO_2 and H_2S in basaltic formations (Gunnarsson, 2013; Ingimundarson, 2015). Field CO_2 injection experiment was conducted in Ogachi HDR geothermal site (Kaieda et al., 2009) by injecting neutralized river water and dry ice in a granitic reservoir to study the feasibility of the reservoir for carbon storage. It is essential to understand the chemical reaction mechanisms taking place as the CO_2-enriched fluid interacts with the reservoir rocks, as these are very important to evaluate the storage capacity of the host rocks: this is to effectively store, trap, and immobilize the injected CO_2 for extended periods of time (Mountain and Higgs, 2015). The properties of both rock and fluid will be altered upon sufficient contact, and how these properties are altered depends on: the target rock mineralogy, permeability, fluid composition, temperature, pressure, and duration of contact (Browne, 1978).

A growing number of experiments and numerical simulation studies are being conducted to explore the mechanisms and reactions prevalent in rock-fluid-CO_2 environments. Mountain and Higgs (2015) performed a flow-through laboratory experiment wherein sandstone is reacted with distilled water and synthetic brine under conditions common to Kupe South oil and gas field, New Zealand. In their experiments, dissolved CO_2 was injected into a sample of sandstone inside a pressure vessel. Similar set-up was also used by Torres and Aqui (2015) to investigate the interaction between andesite and Wairakei condensates while Sonney and Mountain (2013) investigated interaction between greywacke and distilled water and Wairakei reinjection brine. Torres and Aqui (2015) observed dissolution of quartz and feldspar, while secondary minerals anhydrite, chlorite, smectite, and zeolite, and most likely plagioclase precipitated out of solution at higher temperatures. Dissolution is considered to be the predominant process and caused permeability enhancement in their rock samples. On the other hand, Sonney and Mountain (2013) reported that, at room temperature, carbonate containing minerals dissolved through contact with either fluid, and elevated concentrations of Ca, Mg, and Sr were detected accompanied by an increase in pH. However a rapid decrease in pH was observed after the temperature was increased, indicating initial precipitation of secondary aluminosilicates, then a steady-state between dissolving primary minerals and precipitating secondary minerals. Other similar laboratory scale experiments are listed in Table 1.

Table 1. An overview of laboratory scale experiments of CO_2-water-rock interactions.

Reference	Temperature (°C)	Pressure (MPa)	Length (days)	Initial Solids	Aqueous Fluid	Alteration
Bischoff & Rosenbauer, (1996)	200 and 350	50	84-124	rhyolite (ryodacite)	CO_2 - water	dissolution of feldspar
Shiraki & Dunn, (2000)	80	16.6	164 hrs	Sandstone	CO_2 + synthetic reservoir brine	dissolution of dolomite; K-feldspar to kaolinite
Kaszuba et al., (2003)	200	20	139	Arkose	supercritical CO_2 - brine	smectite precipitation
Ueda & K., (2005)	200	2-6	15	granodiorite and plagioclase	DI water w/ supercritical CO_2	calcite and kaolinite precipitation
Suto et al., (2007)	100-350	250	7	Granite	CO_2 - water	kaolinite, muscovite, smectite, calcite precipitation
Credoz et al., (2009)	80 and 150	15	30-365	sandstone and limestone	supercritical CO_2 + synthetic brine	dissolution of carbonates, kaolinite; destabilization of illite/smectite
Lin et al., (2008)	100	15	2	Granite	supercritical CO_2	calcite , aluminosilicate precipitation
Wigand et al., (2008)	60	15	63	Sandstone	supercritical CO_2 + synthetic brine	dissolution of dolomite, K-feldspar and albite
Fischer et al., (2010)	40	5.5	105	quartz and plagioclase	CO_2 + synthetic brine	dissolution of plagiooclase, K-feldspar and anhydrite; formation of albite
Holubnyak et al., (2011)	80	14.5	28	dolomite (60-75%)	10% wt NaCl	dissolution of carbonates
Sonney & Mountain, (2013)	210	3.5	41	Greywacke	re-injection brine	formation of clay minerals
Luhmann et al., (2014)	100	15	61 min - 9 days	dolomite	CO_2 + synthetic brine	dissolution of dolomite
Torres & Aqui, (2015)	230	20	42	Andesite	Wairakei, steam condensate	dissolution of quartz and feldspar; deposition of anhydrite chlorite and zeolites

Effects of CO_2 reinjection is also modelled by using reactive transport modeling. According to Xu and Pruess (2010), for the case of CO_2 injection into a rock mainly composed of altered granite; calcite, K-feldspar and chlorite are dissolved, while dolomite, siderite and ankerite are precipitated and the mineral alteration resulted in a net decrease in porosity of the reservoir. However, Xu et al. (2010) showed that co-injection of water with supercritical CO_2 resulted in strong porosity enhancement by dissolution of calcite, while sequential injection of CO_2 and water brought about a very small porosity enhancement.

Co-injection of CO_2, H_2S, and SO_2 gases into an arkose formation was also investigated by Xu et al. (2007). CO_2 sequestration occurred by precipitation of secondary carbonates calcite, ankerite, and dawsonite, with most of the deposits forming beyond the acidified zone (100 m away from the wellbore). Co-injection of H_2S brought about precipitation of pyrite while SO_2 co-injection resulted in precipitation of pyrite, anhydrite, and alunite; both occurring within the acidified zone. Significant changes in porosity occurred within this acidified zone, where mineral dissolution dominates.

Beni et al. (2012) simulated the reaction of Bunter sandstone formation, which is mainly composed of quartz, K-feldspar, mica, chlorite and kaolinite with brine and CO_2. Water-rock interaction resulted into the alteration of aluminum silicates and precipitation of secondary carbonates (dawsonite, ankerite, and siderite). Porosity was also significantly decreased to 9% of the initial value. Effects of CO_2 gas injection in an enhanced geothermal system (EGS) in the Songliao Basin, China was studied by Na et al. (2015). Laboratory experiments and numerical modeling using the TOUGHREACT code (Xu et al., 2011) were conducted under reservoir conditions (160 ^oC and 35MPa) for 12 days. Numerical simulations were partly successful in reproducing experimental results and show an increase in HCO_3^- , Ca^{+2}, K^+, Fe^{+2}, and SiO_2 (aq) concentration, coupled with a decline in pH, consistent with dissolution of primary minerals. Precipitation of secondary carbonates calcite and ankerite was also observed.

Shevalier et al. (2011) and Dalkhaa et al. (2013) set up a 1-D and 2-D model for CO_2 injection in a saline aquifer that contains H_2S using TOUGHREACT. Nisku carbonate formation which is mainly composed of dolomite (>80%) and calcite (16%) was reacted with brine containing CO_2 and H_2S. The presence of dissolved H_2S did not have significant effect on water-rock interaction. Significant dissolution of dolomite resulted in the increase in porosity by ~0.2%.

In this paper a reactive transport model was created to simulate a laboratory scale experiment (Passarella et al., 2015) of geothermal brine containing high concentration of dissolved CO_2 and H_2S and rock interaction. The rock sample is greywacke, which is a representative lithology of some of the reinjection aquifers in the Taupo Volcanic Zone (TVZ). The laboratory experiment focuses on interactions between unaltered (fresh) greywacke and fluid under geothermal reservoir pressure and temperature conditions. The aim of this study is to recreate experimental analogues of the geochemical processes occurring during re-injection. This thermochemical flow modelling will be used to assess the reaction rates and investigate their effects on porosity and permeability of the rock sample. TOUGHREACT simulator was used, with the fluid property modules ECO2N and EOS1, to account for the effects of chemically reactive fluids in porous and fractured media in non-isothermal flows. PyTough (Wellmann et al., 2012) software was used for model set up and data processing.

2. MODELING OF LABORATORY SCALE NCG-WATER-ROCK INTERACTION EXPERIMENT

2.1 EXPERIMENTAL DESIGN

The model was based on the results of the flow-through experiment conducted by Passarella et al. (2015). This experiment was designed following the set-up of Mountain and Higgs (2015), Torres and Aqui (2015) and Sonney and Mountain (2013) (see Figure 1). A rock sample from the Waotu quarry southeast of Hamilton, New Zealand was used in the experiment. This is similar to greywacke that comprises the basement rock in which re-injection of brines is occurring in some of the geothermal systems in the TVZ. It consists of clasts of siltstone, basalt, quartz, plagioclase, pyroxene and hornblende in a matrix of quartz, feldspar, chlorite, illite, calcite and pyrite. The fluid to which it comes into contact is a mixture of low pressure separator brine from a New Zealand geothermal power station. A synthetic NCG mixture containing $CO_2/H_2S/H_2$ in the ratio of 96%/4%/0.1% is added to this brine.

The experiment was carried out following these steps:

1. The rock sample is coarsely-crushed in a roller mill, sieved to obtain the 355 – 500 μm mesh size, and cleaned several times in an ultrasonic bath in distilled water to remove fine particles. The mineral composition of the unreacted rock was not measured, thus it was assumed based on the modal composition of basement greywacke drill cuttings at Ohaaki (Wood et al., 2001) and XRD analysis of "fresh" greywacke used by Sonney and Mountain (2013). The clean sample is put in a titanium pressure vessel and placed inside an insulated oven. The unreacted rock was analyzed with X-ray diffraction spectrometer (XRD) and scanning electron microscopy (SEM) for comparison with the reacted grains collected after the experiment.

2. 800 mL of de-oxygenated brine from Wairakei power station was drawn into the accumulator and compressed with 200 mL synthetic gas mixture containing $CO_2/H_2S/H_2$ (96%/4%/0.01%) at 35 bar. At first, complete mixture of the brine and NCG mixture was not attained, and the accumulator had to be inverted to allow complete homogenization of the fluid mixture. The brine-NCG mixture was not analysed for its chemistry due to the high pressure (laboratory analysis normally done at atmospheric pressure, will yield different values due to exsolution of gas).

3. Gas enriched fluid was pumped at 1.0 ml hr^{-1} into the pressure vessel at room temperature for 6 days.

4. The temperature was then increased to 200 ^{o}C and maintained for another 60 days. Flow rate was reduced to 0.5 ml hr^{-1} at 38 days into the experiment, in order to test for equilibrium conditions. The temperature is monitored by a thermocouple inserted at the top of the pressure vessel. The fluid pressure is maintained by a back pressure regulator.

5. During injection, water and gas samples are collected daily and analysed in bulk after the experiment. The effluent was analysed for Li, Na, K, Mg, Ca, Sr, Mn, Fe, As, Al, B, SiO_2, Cl^-, and SO_4^-. CO_2 was analysed by back titration and H_2S by methylene blue reaction. XRD and SEM were used to characterize mineral and chemical composition of the reacted rock samples and compared with the unreacted samples.

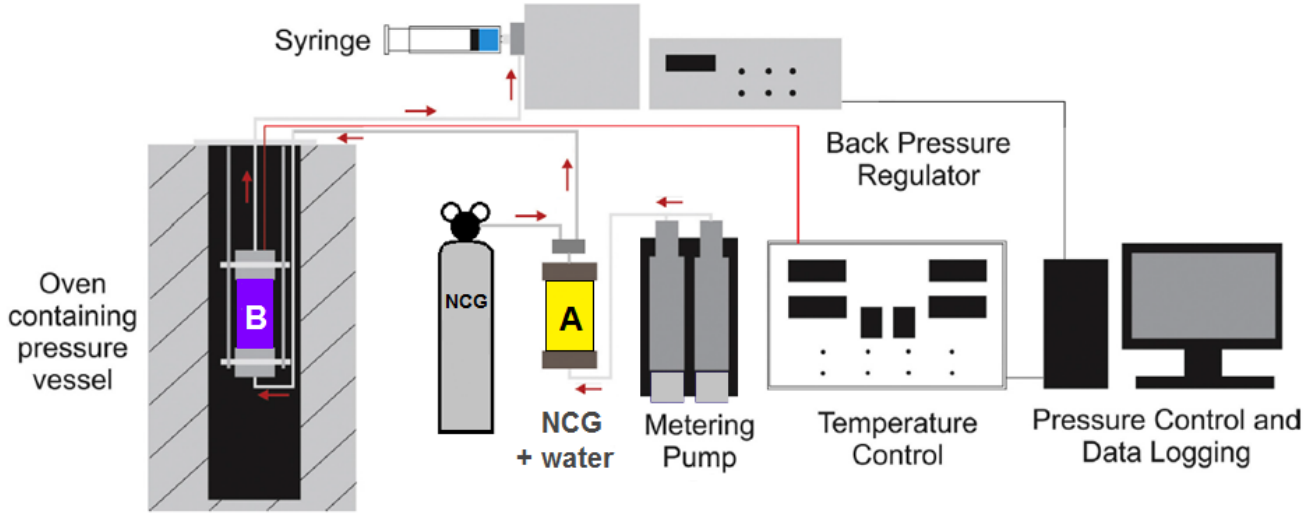

Figure 1. Experimental set-up (modified from Mountain and Higgs, 2015).

More details on the experimental set-up and results are described in Passarella et al. (2015). The purpose of this study is to replicate these experimental results in a reactive model in order to identify key chemical process and quantify the porosity and permeability changes.

In order to perform numerical modelling analyses, two models were developed to represent different stages of the experiment:

a) NCG-Brine mixing and equilibration (shown with yellow in Figure 1) by using ECO2N module;

b) Fluid –rock interaction at high pressure (35 bar) vessel (shown with purple in Figure 1) at 25°C for six days, then at 200°C for 60 days by using EOS1 module.

2.2. MODEL PARAMETERS

2.2.1. NCG-BRINE MIXING AND EQUILIBRATION

In order to represent the conditions for dissolution of synthetic NCG in brine in the accumulator (Figure 1), first a 1 m^3 batch chemical reaction model was set up, by using TOUGHREACT ECO2N module. This model will provide the chemistry of the NCG saturated fluid composition after equilibration between the brine and the synthetic gas mixture, which will then be used in the fluid rock interaction model. It is a single block model, with no generators and no heat flow. The initial fluid concentration for the Wairakei brine sample is listed in Table 2. Inside the accumulator brine will react only with the synthetic gas mixture (96% CO_2/4% H_2S) to reach equilibrium while there is no interaction between fluid and rock.

According to Passarella et al. (2015), 200 ml of synthetic gas reacts completely with 800 ml brine to form a homogeneous mixture. This was implemented in the model by assuming that all CO_2 and H_2S dissolve into HCO_3^- and SO_4^{-2}, respectively. The additional moles of HCO_3^- and SO_4^{-2} are computed, assuming the Ideal Gas Law holds. A mixing model will still be run to account for speciation of these "dissolved" gases. Because the initial brine-synthetic gas mixture was not analyzed, pH was assumed to be equal to that of the fresh brine sample.

Table 2. Initial fluid composition for Wairakei brine sample and results of mixing model

Chemical Parameter	Initial brine composition		Equilibrated totally dissolved gas
	(mg kg^{-1})	(mol kg^{-1} H_2O)	(mol kg^{-1} H_2O)
pH	5.0		5.0
Na^{+}	736.54	3.22E-02	3.20E-02
K^{+}	213.83	5.50E-03	5.47E-03
Ca^{+2}	3.61	9.06E-05	9.01E-05
Mg^{+2}	0.05	1.96E-06	1.95E-06
Fe^{+2}	0.86	1.54E-05	1.53E-05
AlO_2^{-}	0.9	3.36E-05	3.34E-05
Cl^{-}	1747	4.94E-02	4.91E-02
HCO_3^{-}	<20	3.29E-04	3.39E-01
$SO4^{-2}$	96	1.00E-03	9.98E-04
SiO_2 (aq)	1121.44	1.88E-02	1.87E-02
As	3.23	4.33E-05	4.30E-05
B(aq)	36.59	3.40E-03	3.38E-03
Li^{+}	9.5	1.38E-03	1.38E-03
Mn^{+}	0.04	7.82E-07	7.78E-07
CO_2(aq)	NA	NA	3.20E-01
H_2S(aq)	NA	NA	NA

2.2.2. FLUID –ROCK INTERACTION MODEL

A NCG-brine–rock interaction model was set up in order to represent the chemical reactive behavior of the sample at high pressure (35 bar) vessel (shown with purple colour in Figure 1).

Geometry : The model is based on the dimensions of the experimental set-up, and is radial, of 150mm length and radius of 6.25mm (Figure 2). This is discretized into 10 radial grid blocks and 22 layers.

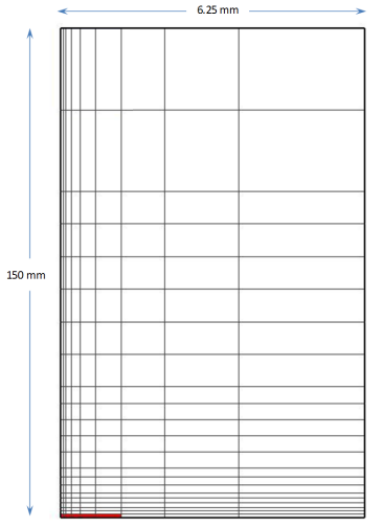

Figure 2. Flow model grid structure. Radial axis is scaled with respect to the vertical axis. Red blocks represent sources.

Initial and boundary conditions: Generation blocks, representing the injection of experimental fluid below the pressure vessel, are assigned to the seven blocks closest to the center at the bottom-most layer (blocks colored in red in Figure 2). A large volume topmost block was considered in order to maintain constant pressure (35 bar) and temperature (25°C and 200°C) conditions.

Initial geochemical conditions: The initial mineral composition of a representative sample of greywacke formation used in the modelling is shown in Table 3. Table 4 lists the parameters assigned to each of the grid blocks assuming the composition of the rock is uniform. The porosity and permeability were estimated from experience, but for the changes in the permeability due to reaction, a simplified form of the Kozeny-Carman equation was used (Xu et al., 2011). The parameters used to determine the kinetic rate constants

of the minerals are given by Palandri and Khalaka (2004) and in the study by Xu et al (2011). Smectite, pyrite, and magnetite, observed in the reacted grains during the laboratory experiment, were included in the model as secondary minerals. Kaolinite, illite, magnesite, dolomite, dawsonite, ankerite, siderite, albite, anhydrite were also considered, as these are likely to be precipitated in very small amounts, and thus, may not have been observed during petrographic analysis of the reacted rock samples.

The results obtained from the mixing model were used for the boundary water composition (Table 2). For the initial water composition, chemical solution of distilled water was used.

Table 3. Initial mineral volume fractions

Mineral	Volume % of Solid
Quartz	40
Oligoclase	13
K-feldspar	5
Calcite	5
Chlorite	1
Non-reactive	36

Table 4. Flow model parameter values

Parameter	Assumed Values	Reference
Permeability, m^2	1.0×10^{-12} (isotropic)	from experience
Porosity	0.40	from experience
Density, kg m^{-3}	2650	Hatherton and Leopard; 1964, Reyes, 2007
C_{wet}*, W $m^{-1o}C^{-1}$	2.5	Eppelbaum et al., (2014)
Specific Heat*, J $kg^{-1o}C^{-1}$	920	Reyes, (2007); Eppelbaum et al., (2014)
Pressure, bar	35	Passarella et al. (2015)
Temperature, ^oC	200	Passarella et al. (2015)

* wet heat conductivity and specific heat of sandstone were used as proxy

2.3 NUMERICAL MODELING OF THE EXPERIMENT AND MODEL RESULTS

Numerical modelling analyses were performed for the model described in Section 2.2.2, by using EOS1 flow module of TOUGHREACT, which considers water, or two waters with typical applications to hydrothermal problems, and heat. Models were run at 35 bar, for six days at room temperature (25°C) and 60 days at 200 °C. Considering there is no significant reaction at low temperature, apart from calcite dissolution, we only present the simulated results for the 200°C temperature case. The simulation results are compared with the data obtained from the experiment.

Most of the activity occurs 10-15mm from the point of injection, characterized by intense dissolution of calcite and chlorite, precipitation of supersaturated minerals quartz, k-feldspar and oligoclase, and formation of secondary minerals smectite, illite, kaolinite, albite, siderite, and ankerite. Overall, an improvement in porosity and permeability was observed close to the point of injection whereas a very slight decline was noted at the upper half of the length of the pressure vessel.

The solubility of quartz at 200^{o}C is 200 mg kg^{-1} (Fournier, 1977). The concentration of silica in the solution (Table 2) is significantly higher than the equilibrium quartz solubility at this temperature, and because the brine was initially supersaturated with silica, quartz deposition was observed. Calcite was shown in Figure 3 to have the most significant change in volume fraction. The dissolution of calcite is due to the low pH, thus, favoring the forward reaction of equation 3. On the other hand, oligoclase which is also supersaturated in the brine, deposits near the point of injection and is stripped of the fluid as it travels up the column (in which case it dissolves into the solution).

Mg^{+2} and Fe^{+2} in the solution increased slightly with the dissolution of chlorite but declined over time as a result of siderite deposition and clay formation (Figure 4 and Figure 5). Precipitation of siderite ($FeCO_3$) is described by Equation 4 as a product of the reaction between Fe^{+2} and HCO_3^-. This is in contrast to experimental observations which instead confirm the presence of pyrite (FeS_2) in reacted rock samples upon conducting SEM-ESD and XRD. This is the result of the representation of H_2S as SO_4- during the mixing model run.

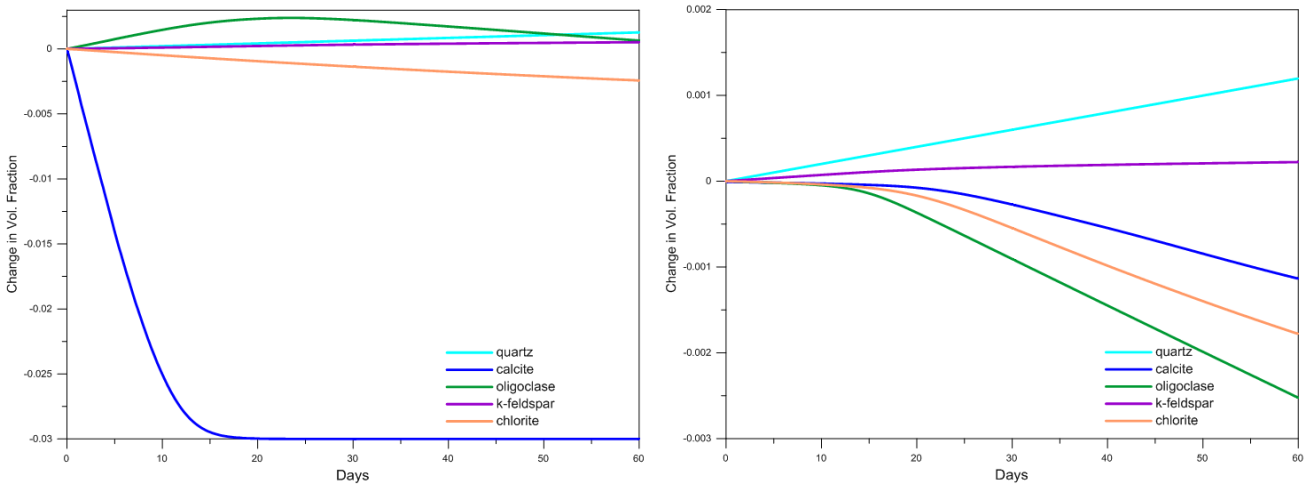

Figure 3. Change in volume fraction of the primary minerals at bottom-most (left) and top (right) blocks of Figure 2.

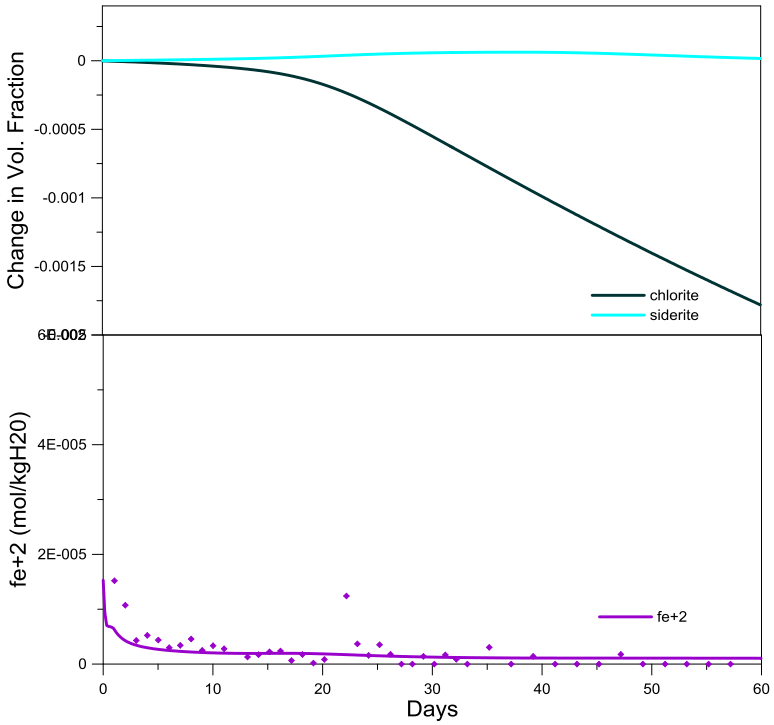

Figure 4. Dissolution of chlorite and precipitation of siderite at top-most block vs. Fe^{+2} concentrations in the solution.

$$CaCO_3 + H^+ \rightleftharpoons Ca^{+2} + HCO_3^- \quad (3)$$

$$Fe^{+2} + HCO_3^- \rightleftharpoons FeCO_3(siderite) + H^+ \quad (4)$$

Figure 5 shows formation of secondary clays illite, smectite-Ca, smectite-Na, and kaolinite which explains the decline in Mg^{+2} concentrations. K^+, Na^+, Ca^{+2}, SiO_2 and Al^{+3} were also consumed, however, the total concentration did not change since these were also regenerated due to the dissolution of primary minerals (Figure 6). Note that in Figure 6, the steep drop in measured silica concentration after 7 days was explained by Passarella et al., (2015) to be a result of silica scaling in the experimental apparatus and should not be matched. Also the declining trend of the measured concentrations of Na^+, K^+, and SiO_2 toward the end of the experiment was brought upon by the leak in the pump piston, allowing distilled water to dilute the brine. pH remains buffered throughout the experiment (Figure 7).

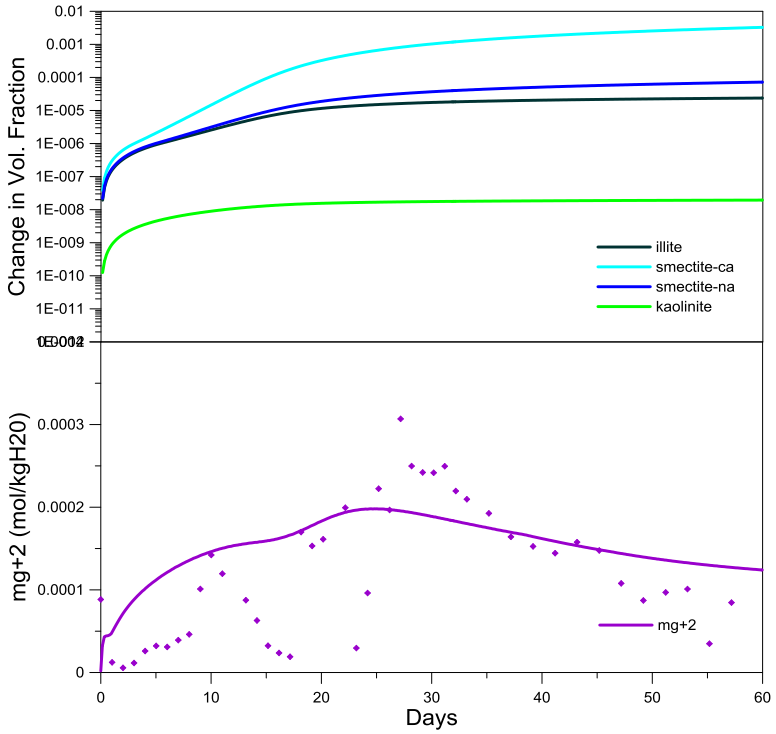

Figure 5. Precipitation of secondary minerals at top-most block vs Mg^{+2} concentration in solution.

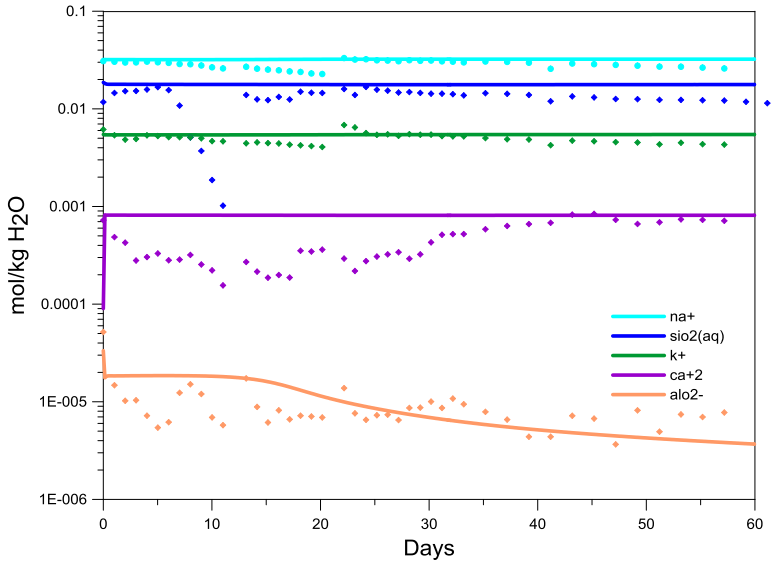

Figure 6. Concentration of major cations at top-most (outlet) block of the model.

A net increase in the porosity and permeability was observed in the simulation. Figure 8 shows that much of the change in porosity and permeability occurred near the injection point, as do other changes such as dissolution of primary minerals and precipitation of clays. Primary mineral dissolution appears to be the primary mechanism near the point of injection while secondary mineral deposition dominates at the upper half of the pressure vessel. Looking at these changes, there still appear to be a net increase in porosity and permeability in the rock sample.

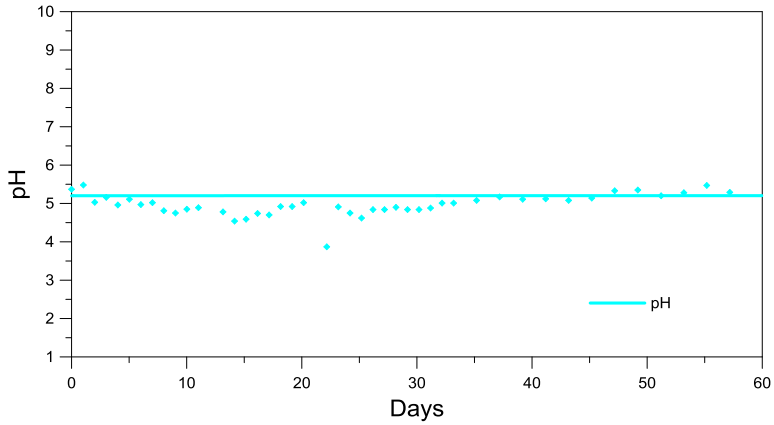

Figure 7.pH trend with time at top-most (outlet) block

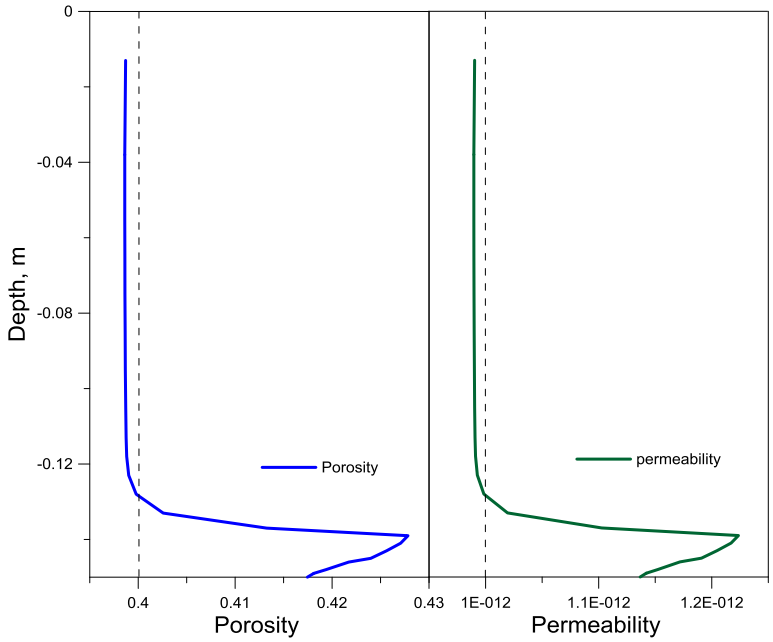

Figure 8. Permeability and porosity change at the end of model run (60 days) vs sample height

Passarella et al. (2015) noted significant dissolution of the ferromagnesian mineral phases. Dense pyrite coatings (confirmed by XRD analysis) were observed in close proximity to corroded ferromagnesian phases including chlorite and pyroxene clasts, indicating relatively fast reaction rates. As mentioned earlier, an improvement of the model will call for the appropriate representation of H_2S in the mixing model in order to allow replication of pyrite deposition, instead of siderite. Therefore, the model was modified with one significant difference: H_2S was assumed to dissolve as HS^- instead of SO_4^{-2}. Another iteration of pyrite was also chosen from the thermodynamic database. The result is given in Figure 9. The pyrite model still showed dissolution of chlorite, however, pyrite is now seen precipitating instead of siderite. The matches for the other mineral and aqueous species were adversely affected, however, in particular more intense chlorite dissolution and less calcite activity is observed. This resulted in higher Mg^{+2} concentrations compared with measured values and faster consumption (decline) of Fe^{+2}.

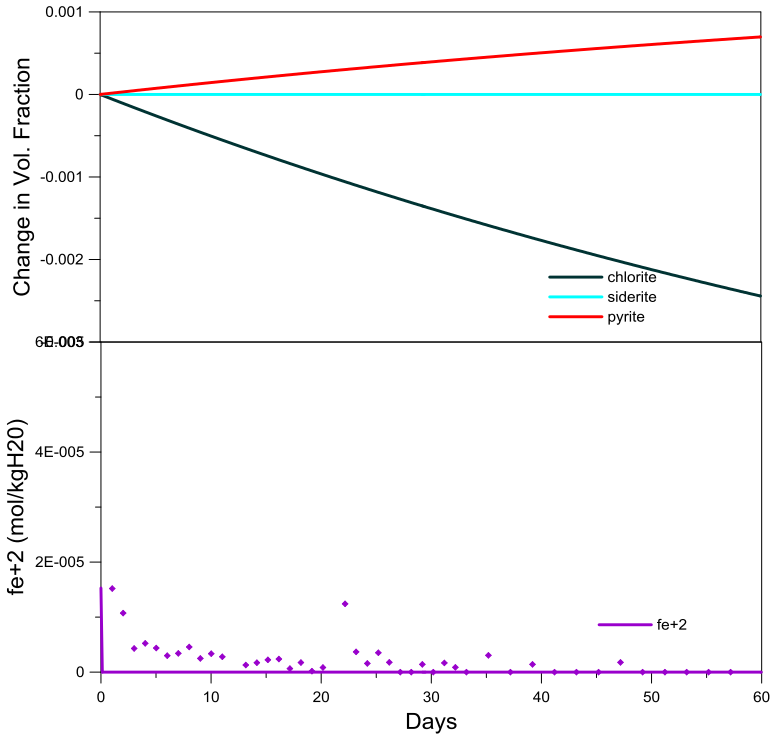

Figure 9. Dissolution of chlorite and precipitation of pyrite and siderite at the top block vs. Fe^{+2} concentrations in solution, pyrite model.

5. CONCLUSIONS AND RECOMMENDATIONS

Experiments were conducted to investigate the interaction between greywacke rock, Wairakei brine and representative synthetic NCG, to assess the reaction rates and evaluate its viability for long term NCG sequestration and permeability enhancement. Numerical simulations were conducted using TOUGHREACT to model: (1) mixing and speciation of CO_2 and H_2S in the brine sample; (2) pumping of brine-gas mixture into the rock substrate at reservoir temperature and pressure conditions.

The mixing model was constructed to obtain initial chemical composition of the brine-NCG mixture, in the absence of measured data. This was done by assuming complete dissolution of CO_2 and H_2S into HCO_3^- and $SO4^{-2}$, respectively. Considering there is no significant reaction at low temperature, apart from calcite dissolution, more emphasis was given to the simulation of the 200°C temperature conditions.

The reactive flow model simulation results show deposition of both quartz and feldspar, which are supersaturated in the injected brine, and dissolution of calcite, oligoclase, and chlorite. The fluid pH appears to have been buffered by the mineral reactions as the dissolution of calcite did not cause any change in pH. Secondary clays were also formed, as well as siderite which is a carbonate mineral. Since the siderite precipitation disagrees with the experimental observations, a separate model was set-up by changing the reaction parameters in the input files. This resulted in the precipitation of pyrite but affected the matches with the other aqueous species.

There is a net increase in porosity and permeability, which diminishes as one goes further out from the injection point. Among the carbonate phases considered in the model, only siderite and ankerite precipitated in very minute amounts. This suggests a degree of sequestration of dissolved CO_2 into the mineral phase, however, Xu et al. (2007) have showed that the alteration of primary minerals and precipitation of secondary carbonates occur at time frames over 100 years and may not be observed during experimental studies. The results of this simulation can be applied on a larger scale, with larger mass injection, and longer duration to see the long term effect of CO_2 injection in geothermal reservoirs.

The results of these simulations reflect the results of the experiment and provide valuable insights into the consequences of injecting brine-NCG mixture into a geothermal reservoir. These results are, however, constrained by the limitation of current reactive transport simulators in representing all complex physical, hydrological, and geochemical processes occurring within the geothermal system, making data fitting between simulated and experimental results very challenging.

REFERENCES

Alfredsson, H. A., & Gislason, S. R. (2009). CarbFix – CO_2 sequestration in basaltic rock: chemistry of the rocks and waters at the injection site. Hellisheidi, SW-Iceland. *Goldschmidt Conference Abstracts*, A26.

Beni, A., Kuhn, M., Meyer, R., & Clauser, C. (2012). Numerical modeling of a potential geological CO_2 sequestration site at Minden (Germany). *Environmental Modeling & Assessment, 17*(4), pp. 337-351.

Bischoff, J. L., & Rosenbauer, R. J. (1996). The alteration of rhyolite in CO_2 charged water at 200 and 350°C: The unreactivity of CO_2 at higher temperature. *Geochimica Et Cosmochimica Acta, 60*(20), pp. 3859-3867.

Bloomfield, K. K., Moore, J., & Neilson Jr., R. (2003). Geothermal energy reduces greenhouse gases. *Bulletin. Geothermal Resources Council, 32* (2), pp. 77-79.

Browne, P. R. L. (1978). Hydrothermal alteration in active geothermal fields. *Annual Review of Earth and Planetary Sciences*, *6*, pp. 229-250.

Credoz, A., Bildstein, O., Jullien, M., Raynal, J., Pétronin, J., Lillo, M., Pozo, C., & Geniaut, G. (2009). Experimental and modeling study of geochemical reactivity between clayey caprocks and CO_2 in geological storage conditions. *Energy Procedia, 1*(1), pp. 3445-3452.

Dalkhaa, C., Shevalier, M., Mayer, B., & Nightingale, M. (2013). 2-D Numerical modeling of CO_2 storage in the Devonian H2S containing Nisku aquifer in the Wabamun Lake Area (Alberta, Canada). *Energy Procedia, 37*, pp. 5331-5338.

DiPippo, R. (2012). Geothermal power plants principles, applications, case studies, and environmental impact (3rd ed.. ed.). Amsterdam ; Boston: Amsterdam ; Boston : Butterworth-Heinemann c2012.

Drysdale, D. (2010). Carbon footprint for the Tauhara stage II geothermal development project. The New Zealand Forest Research Institute (SCION), Rotorua.

Eppelbaum, L., Kutasov, I., Pilchin, A. (2014). Applied geothermics. Retrieved from: www.springer.com/gp/book/10.1007%2F978-3-642-34023-9.

Fischer, S., Liebscher, A., Wandrey, M., & CO2SINK Group. (2010). CO_2–brine–rock interaction—first results of long-term exposure experiments at in situ P–T conditions of the Ketzin CO_2 reservoir. *Chemie Der Erde-Geochemistry, 70*, pp. 155-164.

Fournier, R. (1977). Chemical geothermometers and mixing models for geothermal systems. *Geothermics, 5*(1), pp. 41-50.

Global Carbon Capture and Storage Institute Ltd. (2014) The global status of CCS 2014. Retrieved from www.globalccsinstitute.com/publications/global-status-ccs-2014

Gunnarsson, I., Aradóttir, E. , Sigfússon, B., Gunnlaugsson, E., & Júlíusson, B. (2013). Geothermal gas emission from Hellisheiði and Nesjavellir Power Plants, Iceland. *Transactions, Geothermal Resources Council, 37* (2) pp. 785-789.

Hamidreza, N. M., Wolf, K. H., & Bruhn, D. (2015). Mixed CO_2-water injection into geothermal reservoirs: a numerical study. *Proceedings World Geothermal Congress,* 2015.

Hatherton, T., & Leopard, A. E. (1964). The densities of New Zealand rocks. *New Zealand Journal of Geology and Geophysics*, *7*(3), pp. 605-625.

Holm, A., Jennejohn, D., & Blodgett, L. (2012). *Geothermal* energy and greenhouse gas emissions. Geothermal Energy Association.

Holubnyak, Y. I., Hawthorne, S. B., Mibeck, B. A., Miller, D. J., Bremer, J. M., Sorensen, J. A., Steadman, E. N., & Harju, J. A. (2011). Modeling CO2–H2S–water–rock interactions at Williston Basin reservoir conditions. *Energy Procedia, 4*, pp. 3911-3918.

Hydrogen Sulphide. Public Health England Centre for Radiation, Chemicals and Environmental Hazards. Toxicology Department, 2009 (ver 1). Retrieved from http://www.gov.uk/government/uploads/system/uploads/attachment_data/file/317495/PHE_Compendium_of_Chemical_Hazards_Hydrogen_Sulphide_v1.pdf

Ingimundarson, A., Arnarson, M., Sighvatsson, H., & Gunnarsson, T. (2015). Design of a H2S absorption column at the Hellisheiði Powerplant. *Proceedings, World Geothermal Congress*, 2015.

Jones, B., & Renaut, R. (1998). *Origin* of platy calcite crystalsin hot-spring deposits in the Kenya Rift Valley. *Journal of Sedimentary Research, 68* (5), pp. 913-927.

Kaieda, H., Ueda, A., Kubota, K., Wakahama, H., Mito, S., Sugiyama, K., Ozawa, A., Kuroda, Y., Sato, H., Yajima, T., Kato, K., Ito, H., Ohsumi, T., Kaji, Y., & Tokumaru, T. (2009). Field experiments for studying on CO_2 sequestration in solid minerals at the Ogachi HDR geothermal site, Japan. *Proceedings 34th Workshop on Geothermal Reservoir Engineering,* 2009.

Kaszuba, J. P., Janecky, D. R., & Snow, M. G. (2003). Carbon dioxide reaction processes in a model brine aquifer at 200°C and 200 bars: implications for geologic sequestration of carbon. *Applied Geochemistry, 18*(7), pp. 1065-1080.

Khasani, Miyazaki, E., & Itoi, R. (2004). Numerical study on effects of CO_2 gas in geothermal water on well characteristics. *Proceedings, 2nd International Workshop on Earth Science and Technology*, 2004.

Lin, H., Fujii, T., Takisawa, R., Takahashi, T., & Hashida, T. (2008). Experimental evaluation of interactions in supercritical CO_2/water/rock minerals system under geologic CO_2 sequestration conditions. *Journal of Materials Science, 43*(7), pp. 2307-2315.

Luhmann, A. J., Kong, X., Tutolo, B. M., Garapati, N., Bagley, B. C., Saar, M. O., & Seyfried, W. E. (2014). Experimental dissolution of dolomite by CO_2-charged brine at 100° C and 150bar: evolution of porosity, permeability, and reactive surface area. *Chemical Geology, 380*, pp. 145-160.

Mahon, W. A. J., McDowell, G. D., & Finlayson, J. B. (1980). Carbon dioxide: its role in geothermal systems. *New Zealand Journal of Science, 23*, pp. 133-148.

Mountain, B., & Higgs, K. E. (2015). Simulation of CO_2-water-rock interaction in sandstone reservoirs using a continuous flow-through reactor [unpublished work].

Na, J., Xu, T., Yuan, Y., Feng, B., Tian, H., & Bao, X. (2015). An integrated study of fluid-rock interaction in a CO_2-based enhanced geothermal basin: a case study of Songliao Basin, China. *Applied Geochemistry 59* (2015), pp. 166-177.

Nagl, G. (2009). Coso Goethermal Field 15 years of successful H_2S abatement. *Bulletin. Geothermal Resources Council,* 2009.

Papic, P. (1991). Scaling and corrosion potential of selected geothermal waters in Serbia. UNU Geothermal Training Programme, 1991.

Passarella, M., Mountain, B., Zarrouk, S., & Burnell, J. (2015). Experimental simulation of re-injection of non-condensable gases into geothermal reservoirs: greywacke-fluid interaction. *Proceedings, 37th New Zealand Geothermal Workshop,* 2015.

Plaksina, T., White, C., Nunn, J., & Gray, T. (2011). Effects of coupled convection and CO_2 injection in stimulation of geopressured geothermal reservoirs. *Proceedings, 36th Workshop on Geothermal Reservoir Engineering*, SGP-TR-191.

Richard, M. A. (1990). The Puna Geothermal Venture Project Power for the Island Of Hawaii. *Geothermal Resources Council Transactions*, Vol 14, Part I.

Pruess, K. (2005). ECO2N: A TOUGH2 fluid property module for mixtures of water, NaCl, and CO_2. Earth Sciences Division, Lawrence Berkeley National Laboratory.

Reyes, A. G. (2007). A preliminary evaluation of sources of geothermal energy for direct heat use. *GNS Science Report* 2007/16.

Salimi, H., Groenenberg, R., & Wolf, K. (2011). Compositional flow simulations of mixed CO_2-water injection into geothermal reservoirs: geothermal energy combined with CO_2 storage. *36th Workshop on Geothermal Reservoir Engineering, Stanford University,* pp. 169-181.

Sanopoulos, D., & Karabelas, A. (1997). H_2S abatement in geothermal plants: evaluation of process alternatives. *Energy Sources, 19*(1), 63-77.

Satman, A., Ugur, Z., & Onur, M. (1999). The effect of calcite deposition on geothermal well inflow performance. *Geothermics, 28* (3), pp. 425-444.

Shevalier, M., Nightingale, M., Mayer, B., & Hutcheon, I. (2011). TOUGHREACT modeling of the fate of CO_2 injected into a H_2S containing saline aquifer: The example of the Wabamum Area Sequestration Project (WASP). *Energy Procedia, 4*, pp. 4403-4410.

Shiraki, R., & Dunn, T. L. (2000). Experimental study on water–rock interactions during CO_2 flooding in the Tensleep Formation, Wyoming, USA. *Applied Geochemistry, 15*(3), pp. 265-279.

Simmons, S., & Christenson, B. (1994). Origins of calcite in a boiling geothermal system. *American Journal of Science*, *294*, pp. 361-400.

Sonney, R., & Mountain, B. (2013). Experimental simulation of greywacke- fluid interaction under geothermal conditions. *Geothermics, 47*, pp. 27-39.

Sung, R., Li, M., Dong, J., Lin, A. T., Hsu, S., Wang, C., & Yang, C. (2014). Numerical assessment of CO_2 geological sequestration in sloping and layered heterogeneous formations: A case study from Taiwan. *International Journal of Greenhouse Gas Control, 20*(0), pp. 168-179.

Suto, Y., Liu, L., Yamasaki, N., & Hashida, T. (2007). Initial behavior of granite in response to injection of CO_2-saturated fluid. *Applied Geochemistry, 22*(1), pp. 202-218.

Torres, M. A. B., & Aqui, A. A. (2015). Experimental fluid-rock interaction simulating reinjection of cooling tower condensate in andesitic-hosted reservoir of Southern Negros Geothermal Field, Philippines.

Truesdell, A., & Nehring, N. (1979). Gases and water isotopes in a geochemical section across the Larderello, Italy, Geothermal Field. *Pure and Applied Geophysics* 1978, *117* (1-2), pp. 276-289.

Ueda, A., Kato, K., Ohsumi, T., Yajima, T., Ito, H., Kaieda, H., Metcalfe, R., & Takase, H. (2005). Experimental studies of CO_2-rock interaction at elevated temperatures under hydrothermal conditions. *Geochemical Journal; Geochem.J., 39*(5), pp. 417-425.

Wellmann, F.J., Croucher, A.,Regenauer-Lieb, K., 2012. Python scripting libraries for subsurface fluid and heat flow simulations with TOUGH2 and SHEMAT. Comput. Geosci. 43, pp. 197–206.

Wigand, M., Carey, J. W., Schütt, H., Spangenberg, E., & Erzinger, J. (2008). Geochemical effects of CO2 sequestration in sandstones under simulated in situ conditions of deep saline aquifers. *Applied Geochemistry, 23*(9), pp. 2735-2745.

Wood, C. P., Brathwaite, R. L., & Rosenberg, M. D. (2001). Basement structure, lithology and permeability at Kawerau and Ohaaki geothermal fields, New Zealand. *Geothermics, 30*(4), 461-481.

Xu, T. (2010). Numerical simulation to study the feasibility of using CO_2 as a stimulation agent for enhanced geothermal systems. *Lawrence Berkeley National Laboratory.*

Xu, T., Apps, J., Pruess, K., & Yamamoto, H. (2007). Numerical modeling of injection and mineral trapping of CO_2 with H_2S and SO_2 in a sandstone formation. *Chemical Geology 242*, pp. 319-346.

Xu, T., & Pruess, K. (2010). Reactive transport modeling to study fluid-rock interactions in enhanced geothermal systems (EGS) with CO_2 as working fluid. *Proceedings, World Geothermal Congress,* 2010*,* pp. 25-29.

Xu, T., Spycher, N., Sonnenthal, E., Zhang, G., Zheng, L., & Pruess, K. (2011). TOUGHREACT Version 2: a simulator for subsurface reactive transport under non-isothermal multiphase flow conditions. *Computers & Geosciences*, *37*, pp. 763-774.

Yanagisawa, N. (2010). Ca and CO2 transportation and scaling in HDR system. *Proceedings World Geothermal Congress*, Antalya, Turkey.